# Event-based runoff and sediment yield dynamics and controls in the sub-humid headwaters of the Blue Nile, Ethiopia

Habtamu Assaye[1, 2] | Jan Nyssen[1] | Jean Poesen[3, 4] | Hanibal Lemma[5] | Derege Tsegaye Meshesha[2] | Alemayehu Wassie[2] | Enyew Adgo[2] | Deribew Fentie[2] | Amaury Frankl[1,6]

[1] Department of Geography, Ghent University, Ghent, Belgium
[2] Department of Natural Resource Management, Bahir Dar University, Bahir Dar, Ethiopia
[3] Department of Earth and Environmental Sciences, KU Leuven, Heverlee, Belgium
[4] Faculty of Earth Sciences and Spatial Management, Maria-Curie Sklodowska University, Lublin, Poland
[5] Department of Hydraulic and Water Resources Engineering, Bahir Dar University, Bahir Dar, Ethiopia
[6] INRAE, AMAP, IRD, CIRAD, CNRS, University Montpellier, Montpellier, France
* Corresponding author: Habtamu Assaye (HabtamuAssaye.Deffersha@ugent.be)

**Short informative:** Soil erosion is a major environmental problem in the humid highlands of Ethiopia. Here, we studied the effect of land use types and management on the runoff and erosion response of micro-catchments. We emphasised the effect of catchment characteristics on the runoff and erosion.

**Running head:** Runoff and erosion response of different land use types and management

## ACKNOWLEDGEMENTS

The authors acknowledge the financial support provided by the VLIR-UOS through the Institutional University Cooperation (IUC) project of Bahir Dar University.

**Abstract**

Land degradation due to soil erosion presents a challenge for sustainable development. We investigated the impact of land use type and land management practices on runoff and sediment yield dynamics in the northwestern highlands of Ethiopia. The study area included 14 zero-order catchments with a surface area ranging from 324 $m^2$ to 1715 $m^2$. V-notch weirs produced from plastic jars were introduced as measuring alternatives that met local constraints. Runoff depth at the weir was registered at 5-min intervals during two rainy seasons in 2018 and 2019. Rainfall was measured using tipping-bucket rain gauges. Runoff samples were collected in 1-L bottles and suspended sediment concentration (*SSC*) was determined. The mean event runoff coefficient ranged from 3% for forests to 56% for badlands. Similarly, the mean annual sediment yield (*SY*) was lowest for forests (0.8 Mg $ha^{-1}$ $yr^{-1}$) and highest for badlands (43.4 Mg $ha^{-1}$ $yr^{-1}$), with significant differences among land use types (14.8 Mg $ha^{-1}$ $yr^{-1}$ in cropland, 5.7 Mg $ha^{-1}$ $yr^{-1}$ in grazing land, and 2.9 Mg $ha^{-1}$ $yr^{-1}$ in plantations). Soil organic matter (*SOM*) reduced runoff and *SY*, necessitating the consideration of agronomic and land management practices that enhance *SOM*. Annual *SY* decreased exponentially with the rock fragment cover (*RFC*). In fields where *RFC* was less than 20%, collecting rock fragments for installing stone bunds resulted in a net increase in *SY*. Rehabilitating badlands and enhancing SOM content in croplands can substantially reduce catchment *SY* and, hence considerably contribute to the sustainability of this type of environment.

**Keywords**

Badlands, rock fragment cover, soil erosion, soil organic matter, stone bunds.

# 1 | INTRODUCTION

Soils provide a wide range of ecosystem services, such as the provision of food and fibre, carbon sequestration, and flood regulation (FAO, 2015). Soil erosion by water (i.e. water erosion) has been identified as the most important soil degradation process globally, threatening food security and sustainable development in many regions, especially in the sub-humid tropics characterised by a steep mountainous topography, erosive rains, and poor land use and management practices (Ebabu et al., 2017; Haregeweyn et al., 2015; Lemma et al., 2019; Nyssen et al., 2015; Wuepper et al., 2020). The off-site effects of soil erosion are considerable, causing flash floods, pollution of water bodies, and rapid sedimentation of lakes and reservoirs (Lemma et al., 2019).

Most studies on water erosion are based on measurements from runoff plots or from large river catchments (Poesen, 2018). Much less information is available on small catchments in headwater areas for which topography, soil, land use, cover, and management are rather homogeneous and, therefore, correspond to land units relevant for tailored land restoration initiatives. A recent study showed that land management interventions such as stone bunds and vegetation rehabilitation on steep slopes have significantly reduced catchment runoff (Assaye et al., 2021). Besides the effect of land use and cover on water erosion dynamics, of particular interest is the effect of land management practices in cropland on soil characteristics (e.g. organic matter content or rock fragment cover; RFC) and their consequent effects on water erosion dynamics. For example, soil organic matter (SOM) content has been shown to have an important impact on catchment hydrology, as it enhances soil structural porosity and hence infiltration capacity (Yimer et al., 2008). The relationship between RFC and sediment yield (SY) can generally be expressed by an exponential decay function (Nyssen et al., 2008; Poesen & Lavee, 1994; Poesen et al., 1994). However, few studies have analysed the effects of these factors on soil erosion in sub-humid tropical environments.

In northwest Ethiopia, as in many other subtropical areas, poor land use and management practices have severely accelerated soil erosion (Borrelli et al., 2017). Growing demands driven by a fast population growth (Bruin et al., 2015; Minale, 2013) have been largely fulfilled in the past by expanding cropland areas at the expense of forests, shrublands, or grazing lands, even on steep slopes (Zeleke & Hurni, 2001). Such conversions have exposed the top soils to erosive rains, resulting in high erosion rates (Wassie, 2020). Consequently, most of the areas affected by

severe soil erosion are associated with very high population densities (Haregeweyn et al., 2017). The loss of fertile topsoil has gradually led to increased soil compaction, and thereby, reduced soil infiltration capacity (Yimer et al., 2008) and an increase in runoff volume. The runoff erosivity further aggravates the rates of soil erosion (Rodríguez-Blanco et al., 2012). Ethiopia accounts for half of the total soil erosion in East Africa, although it covers only 18% of the region's area (Fenta et al., 2020).

The rate of soil erosion in Ethiopia shows a wide range of spatial variability and is among the highest in the world (Haregeweyn et al., 2015; Haregeweyn et al., 2017). In a pioneering study, Hurni (1983) estimated the annual soil loss by water erosion at approximately 1.5 billion Mg, with an average of 42 Mg $ha^{-1}$ $yr^{-1}$ on croplands. Several other studies reported annual soil loss in the range of 6–200 Mg $ha^{-1}$ $yr^{-1}$ (Taye et al., 2013; Adugna, 2015; Adimasu et al., 2014; Bewket and Teferi, 2009), which is much higher than the tolerance limit range of 5–11 Mg $ha^{-1}$ $yr^{-1}$ (Hurni, 1983). The highest rates of soil erosion (up to 79 Mg $ha^{-1}$ $yr^{-1}$) were recorded for the sub-humid environments (Bewket & Sterk, 2003; Steenhuis et al., 2009). Most studies, however, focus on agricultural land, whereas soil erosion in other land use types and with different land management practices is underrepresented. For instance, physical erosion control structures such as stone bunds, terraces, diversion channels, and grassed waterways have been implemented extensively over the last few decades (Abera et al., 2020; Wolka et al., 2018). However, subsequent impact studies were lacking and, hence, actual achievements were not sufficiently recognised and reliable conclusions could not be drawn (Haregeweyn et al., 2015; Tamene et al., 2019).

Therefore, in this study, we investigated the effects of land use type and land management practices on water erosion in the headwater areas of the Lake Tana Basin in sub-humid NW Ethiopia. We do this by considering zero-order catchments, that is, catchments which have no channel and only sporadically produce runoff and SY following rainfall events, but have been overlooked in most watershed and hydrology studies (Storey et al., 2009; Tsuboyama et al., 2000). The specific objectives are: (i) to analyse event-based runoff and SY for zero-order catchments for the major land use types in NW Ethiopia (i.e., natural forests, plantations, croplands, grazing lands, and badlands) and (ii) to identify factors controlling the erosion rates.

## 2 | MATERIALS AND METHODS

## 2.1 | Study area

This study was conducted in the Enkulal catchment (Figure 1; 11°37–11°39' N, 35°46'–37°49' E), representative of the headwaters of the eastern Lake Tana Basin in terms of topography, climate, soil, land use, and management. The catchment drains to the Gumara River, which is a major sediment contributor to Lake Tana (Lemma et al. 2019, 2020). It covers an area of 10.4 $km^2$ with an elevation ranging from 2229 m to 2561 m above sea level (a.s.l.). The average annual precipitation is 1250 mm, and the daily average air temperature ranges from 18 °C to 25 °C (Adem et al., 2017; Temesgen et al., 2014). The geological composition of the catchment consists mainly of basalt, with minor deposits of volcanic ash (ignimbrite) (Poppe et al., 2013). Young soils prevail, with Luvisols and Leptosols being the major soil types (Colot, 2012). In terms of land use, rainfed cropland is dominant, and the main crops cultivated in this area are teff (*Eragrostis teff*), maize (*Zea mays*), barley (*Hordeum vulgare*), wheat (*Triticum aestivum*), pearl millet (*Pennisetum glaucum*), and potato (*Solanum tuberosum*) (Abera, 2017). Grazing lands are found only in small, fragmented parcels, some used for free grazing, and some in a *cut-and-carry* management system. Over the past few decades, eucalyptus trees (mostly *Eucalyptus globulus*) have been widely planted by farmers on fresh or degraded croplands. Land degradation in the area is caused by deforestation, overgrazing, and poor management of the agricultural land (Dessie et al., 2014; Frankl et al., 2019). A wide range of interventions on stone bunds, check dams, trenches, and tree planting have been undertaken recently (MoFED, 2010; NPC, 2015).

**FIGURE 1** ***here***

## 2.2 | Measurement of rainfall and antecedent soil moisture

Five tipping-bucket rain gauges (HOBOware with data logger) were installed (Figure 1), and rainfall was measured automatically during 2018 and 2019. For every rainfall event, the total rainfall depth ($P$, mm) and the maximum 30-min rainfall intensity ($I_{30}$, mm $h^{-1}$) were derived from the continuous rainfall data series (5-min time step). Five-day cumulative rainfall was used as an indicator for antecedent moisture condition (*AMC*).

## 2.3 | Measurement of runoff and sediment yield

Fourteen catchments (324–1715 $m^2$) draining to first-order streams or gullies were selected for this study (Table 1) to represent the observed variability in land use and management. A

minimum of two catchments were selected from each land use type to represent the differences in controlling factors. The outlet of each catchment was equipped with a V-notch weir, locally made from plastic jars as a less sensitive alternative to theft. During rainfall events, the runoff stage from the weir crest was recorded at 5-min intervals, and the runoff discharge was calculated using Eq. 1 (Shen, 1981):

$$Q = \frac{8}{15} x\, C_v x \sqrt{2g} \times \tan\left(\frac{\theta}{2}\right) x\, h^{\frac{5}{2}}, \quad (1)$$

where $Q$ is the runoff discharge ($m^3\ s^{-1}$), $C_v$ is the discharge coefficient (0.593 for a 90° V-notch), $\theta$ = 90° is the notch angle, $g$ is the acceleration due to gravity ($m\ s^{-2}$), and $h$ is the stage height (m).

Then, the event runoff volume ($RO_v$, $m^3$) and runoff depth ($RO_d$, mm) were determined using Eqs. 2 and 3, respectively.

$$RO_v = \sum_{i=1}^{n} Q_i * t_i, \quad (2)$$

$$RO_d = 10^3 * RO_v / A \quad (3)$$

where $Q_i$ is discharge ($m^3\ s^{-1}$), $t$ is time (s), which is 300 s for 5 min, $A$ is the catchment area ($m^2$), and $i$ is the specific 5-min time step.

The event average suspended sediment concentration (*SSC,* $g\ l^{-1}$) was determined by taking a composite sample of one L taken during the flow rising, peak, and recession times in 2018. However, it was not possible to develop a rating curve from the composite samples; hence, in 2019, 1 L sample was taken during each event at about the peak time. The runoff samples were filtered using Whatman filter paper 42, and *SSC* was determined following the standard laboratory method (Gray et al., 2000). Then, the *SSC* to *Q* rating curve was developed (Table 3), and the event sediment yield (*SY*, Mg) was determined using Eq. 4.

$$SY = \sum_{i=1}^{n} SSC_i * Q_i ¿ t_i, \quad (4)$$

Therefore, the event-weighted average *SSC* was determined using Eq. 5.

$$SSC = SY / RO_v, \quad (5)$$

Then, runoff depth (mm), runoff coefficient (*RC* in%, that is a fraction of rain depth that runs off), *SSC*, and *SY* were determined for each rain event. In addition, a rating curve was developed for the event rainfall depth and SY (Annex A) which was used to estimate the SY for night-time events and hence, annual SY.

**FIGURE 2** ***here***

**2.4 | Physical characterisation**

Each catchment was delineated, and its surface area was determined using a geographic positioning system (GARMIN handheld GPS) and ground surveying techniques (https://www.civilknowledges.com/chain-surveying/). The slope gradient was measured using a clinometer on a representative section of the catchment, mostly from bottom to top. RFC was determined by laying a 1 m × 1 m square grid (Gong et al., 2018; Poesen & Lavee, 1994) that was photographed perpendicularly. Subsequently, a square mesh (20 × 20 mesh with 5 cm × 5 cm units) was overlaid over the photo of the square grid, and rock fragments covered by mesh units (25 $cm^2$) were counted on a computer screen; the rock fragment cover (*RFC, %)* was calculated using Eq. 6.

$$RFC = \frac{Nms}{400} x\,100\,\%, \quad (6)$$

where $N_{ms}$ is number of mesh units with rock fragments.

Mineral fragments with a minimum size of 2 mm were considered as rock fragments (Poesen et al., 1994), and small rock fragments that did not cover a mesh unit (25 $cm^2$) were subjectively added to make up a mesh unit. The *RFC* was also visually estimated in the field for cross-validation of results.

A soil sample was collected from each catchment at a representative position to a depth of 30 cm. Then, *SOM* was determined using the Walkley & Black (1934) method and soil texture was analysed through the hydrometer method (Beretta et al., 2014).

**TABLE 1** ***here***

**FIGURE 3** ***here***

## 2.5 | Data analysis

Event runoff depth, *RC*, and *SY* were compared among the different land use types and seasons using one-way analysis of variance (ANOVA). Correlation coefficients and simple linear regression were used to identify the relationship between catchment characteristics, event runoff, and *SY* of micro-catchments. Principal component analysis (PCA) was used to identify the catchment characteristics associated with runoff and *SY*.

The soil loss tolerance limit for the study area was 6 Mg $ha^{-1}$ $yr^{-1}$ (derived from Hurni, 1983). This annual soil loss tolerance limit was distributed to each event by multiplying the ratio of the event rainfall with the annual rainfall as a weighting factor; hence, the corresponding event threshold *SY* was determined. Then, the *SY* of the observed event and its corresponding threshold were compared to identify events that exceeded the tolerance limit (threshold). Statistical analysis and graphics were performed using R software (R Core Team, 2020).

# 3 | RESULTS

### 3.1 | Event rainfall, runoff, and sediment yield

A total of 3458 rainfall events were measured in the two years in all catchments, which is equivalent to the average of 124 rainfall events per year per catchment. Hence, the runoff was measured for 618 rainfall events (during daytime and when a runoff was generated), which is equivalent to 22 rainfall-runoff events per year per catchment. A summary of the event means *P*, $I_{30}$, and $RO_d$ is presented in Table 2. The average event rainfall varied between 6 mm and 14 mm, and the maximum 30 min intensity ($I_{30}$, mm $h^{-1}$) was from 13.2 to 56 in the different catchments and years.

Runoff responses varied significantly across land use types ($p < 0.01$) (Table 2). The average runoff coefficient (*RC*) in natural forests was the lowest, and that in the badland was the highest. The *RC* of grazing lands was higher than that of cultivated and natural forests. The *RC* of plantation forests showed higher values than that of natural forests, but lower values than that of grazing land (Figure 4a, Annex B). The *RC* response in the different land use types was in the order of BDL > GR > CR > PL > NF (Table 1).

As presented in Figure 4b, the *SSC* of an average event was the highest in the badland and the lowest in the protected grazing land, natural forest, and plantation. The average event *SSC*s from grazing land, natural forest, and plantation forest were significantly smaller than the average event *SSCs* for the other land use types (Table 2). Because of the presence of a footpath that goes through the forest, a higher *SSC* was registered for the forest than grazing land.

The average event *SY* was the highest in the badlands (Figure 4c), whereas intermediate values were observed for croplands. However, the lowest average event *SY* was obtained for the natural forest. The variability for the event *SY* response was the highest in the badlands. Overall, the event average *SY* was higher in 2019 than in 2018 because of the higher rainfall in 2019. In addition, the high *SY* variation between the two years in the croplands could be due to variations in crop type and management (Annex C).

**TABLE 2** ***here***

**TABLE 3** ***here***

**FIGURE 4** ***here***

## 3.2 | Annual sediment yield for the different land use types

The average event *SY* was significantly different among land use types ($p < 0.01$, Annex B). The highest *SY* was observed for badlands, which was significantly higher than that of all other land use types, and the lowest was recorded for the natural forest.

**FIGURE 5** ***here***

The annual *SY* for the croplands varied between 9.4 and 24.7 Mg $ha^{-1}$, which is significantly lower than *SY* for the badlands and higher than *SY* for the grazing lands, natural forests, and plantations. Significant variations were also observed in the different cropland catchments (Figure 5). There was no significant difference among the forests, plantations, and protected grazing lands. The annual *SY* was generally higher in 2019 than in 2018, although the difference was not statistically significant ($p = 0.76$).

**FIGURE 6** ***here***

The cumulative events *P*, $RO_d$, and *SY* for the different land use types are presented in Figure 6. The steepest gradient (grey shaded) indicates the period during which there were high runoff and erosion, observed from mid-July to mid-August. In addition, the cumulative *SY* and runoff were the highest in the badlands and the lowest in the forests. In grazing lands and plantations, the cumulative runoff continues to rise with cumulative rainfall, while the cumulative *SY* remains nearly constant, particularly after the end of August. However, in croplands, the cumulative *SY* continues to rise with rainfall (CR3 and CR4 in particular), indicating that even under a high crop cover, runoff in croplands still causes soil erosion as compared to grazing lands and plantations.

### 3.3 | Factors determining the runoff and erosion processes

#### 3.3.1 | Factors related to the rainfall erosivity agent

The frequency of occurrence of rainfall, *SY*, and $I_{30}$ in the different rainfall classes are presented in Figure 7. The contributions (in %) of the total rainfall in rainfall classes 2 and 3 were

comparable. However, the contribution of *SY* in rainfall class 3 was higher because $I_{30}$ was also higher. Rainfall class 6, which contributed only 2% of the total rainfall, had ~13% of the total *SY*, as the highest $I_{30}$ was observed in this class. In contrast, about half of the rainfall events had a rainfall depth (*P*, mm) of less than 5 mm, but contributed less than 5 % of the total *SY* (Figure 7, Table 4).

**FIGURE 7** ***here***

The correlations between rainfall parameters, antecedent moisture, and runoff are presented in Figure 8. The results show that event $RO_d$ was positively correlated with the corresponding *P* and $I_{30}$. However, the correlation between the antecedent moisture conditions and $I_{30}$ was weak.

**FIGURE 8** ***here***

In Figure 9, event *SY* was presented in relation to event *P* which indicated that in the badlands and croplands, sediment export occurred even during small rainfall events. However, in the forests, grasslands, and plantations, the *SY* response was negligible, and it was only evident during high rainfall events (> 20 mm). The solid line in Figure 9 is the event soil loss tolerance threshold, which is equivalent to the fraction of the annual soil loss tolerance limit weighted by the proportion of the event rainfall to the annual rainfall. Up to 95% of the events in the badlands were above the threshold level, while in the forests, no event was found to have *SY* above the threshold limit (Table 4).

**FIGURE 9** ***here***

**TABLE 4** ***here***

### 3.3.2 | Factors related to catchment properties

The *PCA* results indicated that clay, $RO_d$, and *RC* were strongly and positively associated, while silt and *SOM* were strongly but negatively associated according to the first *PCA* (*Dim 1*, Figure 10). The *SY* was moderately and positively associated with both the first and second *PCAs*. This indicates that the runoff parameters are strongly influenced by soil properties, texture, and *SOM*. The *SOM* was negatively associated with both the $RO_d$ and *SY*. A linear regression on the log-transformed data indicated that small improvements in *SOM* would result in a significant reduction in runoff and *SY* (Figure 10). A dramatic reduction in runoff and *SY* was particularly observed for *SOM* content < 4%, in which the runoff was reduced by approximately 50% and *SY* by ~5 times. Stone *Bund*, *Feses*, and *RFC* (variables with high values in croplands where *SY* was also high) were positively associated with *SY* in the second *PCA*. Slope gradient (*SlopeG*) seems to be less associated with both *PCA*s. However, the total variance explained by the two *PCAs* was only ~57%, and the effect of the slope gradient might show better association in the third component, which explains only ~16% of the variance (Annex G). Slope length (*SlopeL*) showed a strong negative association with the second *PCA*.

The *SY* also showed a declining trend with *RFC*, which was expressed as an exponential decay function (Figure 12). A decrease in the *RFC* from 50% to 40% caused an 11% increase in *SY*. However, a decrease in the *RFC* from 10% to 1% caused a 186% increase in annual *SY*. The effect of *RFC* was more pronounced on annual *SY* than on $RO_d$.

**FIGURE 10** ***here***

**FIGURE 11** ***here***

**FIGURE 12** ***here***

## 4 | DISCUSSION

### 4.1 | Temporal and spatial dynamics of event runoff and sediment yield

Peak runoff and *SY* periods were observed between mid-July and mid-August. This was due to frequent rainfall with the steepest slope of the cumulative rainfall (Figure 6). In addition, the *AMC* was high, triggering the immediate generation of runoff. In addition, July and August are

periods of intensive agricultural activities such as ploughing, weeding, and planting (Annex E) which favour detachment and transport of sediment.

Among the human-induced factors that affect runoff and *SY*, land use change and management play a key role (Poesen, 2018). In this study, a wide range in variations was observed in event runoff and *SY* among the different land use types. The natural forests produced the least amount of runoff and *SY* (Figures 4 and 5), as was the case in other studies (Descheemaeker et al., 2008; Kassa et al., 2019). This is due to the effect of forest interception and a thick litter layer that shields the soil substrate from any form of impact caused by raindrops. Otherwise, concentrated droplets, if falling from big leaves from higher canopy, would in some situations cause higher splash (Wakiyama et al., 2010). In addition, extensive root systems in forests also facilitate rapid rates of infiltration, percolation, and subsurface flow (Farrick & Branfireun, 2014). The runoffs and *SYs* observed from the natural forests in this study are primarily due to the presence of a narrow footpath (approximately 0.5 m × 20 m); otherwise, both runoff and *SY* are close to nil. Forest ecosystems are vital in regulating water balance, reducing surface runoff (Alaoui et al., 2011), and distributing rainwater in different storages (Archer et al., 2016). Leaf litter alone reduces runoff by approximately 30% and *SY* by over 80% (Li et al., 2014). In another study, a 50% plant cover reduced *RC* to below 2% and soil erosion to nil (Sajikumar & Remya, 2015).

In contrast to forests, badlands produced the highest rate of event *RC* and *SY* (Figures 4, 5, and 6), which was supported by additional measurements using exposed tree roots of known age. From 70 exposed tree root depth measurements (tree age ranging from 4 years to 30 years, average 10.1 years; root exposure depth range from 5 cm to 75 cm, average 18.3 cm), the average annual soil erosion rate corresponds to a soil depth of 1.83 cm, which is equivalent to ca. 230 Mg $ha^{-1}$ $yr^{-1}$ (Figure 13), assuming a mean soil bulk density of 1.5 Mg $m^{-3}$. Badlands are, therefore, hotspots of soil erosion but they have not gained sufficient scientific attention in the Lake Tana Basin. High soil erosion rates (200 Mg $ha^{-1}$ $yr^{-1}$) in badlands of the Upper Blue Nile basin (Haregeweyn et al., 2017) as well as in the Mediterranean region (i.e. ca. 250 Mg $ha^{-1}$ $yr^{-1}$ for catchments with similar size as those investigated in this study; Nadal Romero et al. 2014) have also been reported. The lack of vegetation cover and direct exposure of the soil substrate to raindrop impact causes compaction and surface sealing which is exacerbated by soil detachment due to animal trampling. Hence, the rate of infiltration is reduced, causing an increase in runoff

and erosion. While the runoff mechanism in the study area is generally driven by excess in saturation (Tilahun et al., 2015), Hortonian flow can be dominant in the badlands. Low *SOM* content and surface roughness would also favour high-flow shear stresses during runoff events. Finally, as badlands are intensely dissected and severely degraded areas (Nadal Romero et al., 2011), the average local slope is higher than the overall landscape slope.

**FIGURE 13** ***around here***

The soil erosion rate in the region is strongly affected by ongoing land use changes (Temesgen et al., 2014), similar to that in many countries around the world (Msofe et al., 2019). Forests have been converted to croplands in recent decades either through gradual expansion by frontier farmers (Zeleke and Hurni, 2001) or through large-scale private investments commissioned by the government (Teklemariam et al., 2016a). As can be observed from the results of this study (Figures 4, 5, and 6), the event runoff and *SY* were two orders of magnitude higher in the croplands than in the forests. Therefore, the conversion of remaining forests to croplands will significantly aggravate soil erosion and lead to land degradation (Teklemariam et al., 2016b).

In contrast, there is a concerted effort to rehabilitate degraded areas, particularly in the highlands (Abera et al., 2020). Such efforts will play a paramount role in the hydrologic and erosion processes of the area in the long term. In addition, there is a growing trend of converting marginally productive land to eucalyptus woodlots, with log prices increasing constantly (Birhanu & Kumsa, 2018). In our study, the eucalyptus catchments had the second lowest *SY*, next only to natural forests. Therefore, disregarding other ecological effects, it can be concluded that expanding eucalyptus plantations, often in croplands, would reduce soil erosion. Other studies have also found a significant reduction in runoff in eucalyptus woodlots compared to croplands (Mbilinyi et al., 2017). However, as eucalyptus is a controversial tree species with high water consumption and allelopathic effects on other plants (Chanie et al., 2013), warranting further studies to evaluate the water balance, nutrient balance, and long-term effects of expanding eucalyptus plantations on soil health and sustainability.

### 4.2 | Catchment characteristics that control runoff and erosion

RFC significantly reduced the runoff (Figure 12). The *RFC* affects the hydrological process in different ways. If rock fragments are well-embedded in the topsoil, they reduce the infiltration

rate and cause an increase in the surface runoff. However, if rock fragments rest on the soil surface, they enhance infiltration and reduce the surface runoff by reducing flow velocity (Poesen et al., 1998). Taye et al. (2014) found a declining trend in runoff along an increasing slope gradient, which was attributed to a corresponding increase in the *RFC*. Using simulated rainfall, Lv et al. (2019) also found that rock fragments reduced surface runoff and erosion and increased the infiltration of spoil heaps. In addition, Chen et al. (2011) also reported an increasing *RFC* with increasing topographic position.

In our study, the *RFC* was mostly high in croplands where the long-term ploughing action moved rock fragments by kinetic sieving to the soil surface (Oostwoud Wijdenes et al. 1997). In addition, the rock fragments in the grazing lands or plantations were often partly or fully embedded in the soil. This could be an additional reason why the *RC* was higher in grazing lands than in croplands (Figure 4). The *RFC* reduced event runoff and annual *SY*, and the trend was expressed by a negative exponential relation (Poesen & Lavee, 1994; Smets et al. 2008). However, the effect of *RFC* on *SY* was more pronounced when the *RFC* was generally lower. When making stone bunds by collecting rock fragments from the soil surface, it is important to evaluate whether it is better to make stone bunds or to leave rock fragments in the field. Based on our study, it could be inferred that when rock fragments exceed 50%, collecting 10% of rock fragments for making stone bunds would have a net positive effect, as a 10% decrease in the *RFC* will reduce the *SY* by less than 10%, and stone bunds reduce the *SY* by over 30% (Tamene et al., 2019). However, if the rock fragments cover is less than 10%, reducing *RFC* will increase *SY* by over 185%, in which case collecting rock fragments for the construction of stone bunds will result in a net increase in *SY*. Reducing the *RFC* from 20% to 10% increased the *SY* by 27% which is comparable to the gain obtained from constructing stone bunds (Adimassu et al., 2014). Therefore, a 20% stone cover can be set as the lower limit for the trade-off between maintaining *RFC* and constructing stone bunds (Nyssen et al., 2001). However, further investigation is required to obtain a solid and accurate threshold. Studies on the effect of the size and surface arrangement of the rock fragments on *SY* are additionally required.

The SOM increases infiltration and soil water-holding capacity, reduces soil erodibility, and amends soil structure (Olubanjo, 2017). As also observed in our study, a declining *SOM* in croplands to below 2% would dramatically increase *SY* (Figure 12). For soils with < 4% *SOM*,

small improvements would result in a rapid reduction in runoff and *SY*. Therefore, crop residue management and the integration of other vegetative soil and water conservation activities can play a vital role in reducing erosion in the area.

## 5 | CONCLUSION

This study provides deeper insights into event runoff and SY under different land use types in sub-humid tropical highlands. Forests produced the least amount of runoff and the lowest *SY*, whereas badlands were found to be the hotspots of soil erosion. The annual *SY* from croplands shows a large variation (9.8–25.6 Mg $ha^{-1}$ $yr^{-1}$), which is still higher than the soil loss tolerance limit estimated for the area (6 Mg $ha^{-1}$ $yr^{-1}$). However, the estimated mean *SY* from croplands (14.8 Mg $ha^{-1}$ $yr^{-1}$) is generally lower than that in previous studies which could be attributed to the soil and water conservation efforts that have been widely practiced in the area. The year-to-year variations in runoff and erosion responses were not significant. *SOM* was found to be one of the most important parameters that had a profound effect on both event runoff and *SY*. Anthropogenic activities that would reduce *SOM* would therefore worsen the runoff erosion process. Therefore, particular attention is needed in land management activities that contribute to enhancing *SOM*. The relationship between the *RFC* and *SY* was expressed with a negative exponential function which highlighted the need to balance the trade-off between the role of *RFC* when left in the field or collected for bund construction. A 20% *RFC* has been suggested as a threshold below which it is not worth collecting rock fragments from the soil surface to construct bunds. As badlands are found to be hotspots of soil erosion by water, further study is needed on their distribution, causes, and possible remedial measures. They should also be given priority when treating catchments with soil and water conservation measures to reduce the overall catchment *SY*.

**References**


Abera, W., Tamene, L., Tibebe, D., Adimassu, Z., Kassa, H., Hailu, H., … Verchot, L. (2020). Characterizing and evaluating the impacts of national land restoration initiatives on ecosystem services in Ethiopia. *Land Degradation and Development*, *31*(1), 37–52. https://doi.org/10.1002/ldr.3424

Abera, M. (2017). Agriculture in the Lake Tana Sub-basin of Ethiopia. *Social and Ecological System Dynamics*, 375–397. https://doi.org/10.1007/978-3-319-45755-0_23

Adem, A. A., Aynalem, D. W., Tilahun, S. A., & Steenhuis, T. S. (2017). Predicting Reference Evaporation for the Ethiopian Highlands. *Journal of Water Resource and Protection*, *09*(11), 1244–1269. https://doi.org/10.4236/jwarp.2017.911081

Adimassu, Z., Mekonnen, K., Yirga, C., & Kessler, A. (2014). Effect of soil bunds on runoff , soil and nutrient losesm and cropyield in the central highlands of Ethiopia. *Land Degrad. Develop. 25: 554–564*.

Adugna, A. (2015). Soil erosion assessment and control in Northeast Wollega , Ethiopia, 3511–3540. https://doi.org/10.5194/sed-7-3511-2015

Alaoui, A., Caduff, U., Gerke, H. H., & Weingartner, R. (2011). Preferential Flow Effects on Infiltration and Runoff in Grassland and Forest Soils. *Vadose Zone Journal*, *10*(1), 367–377. https://doi.org/10.2136/vzj2010.0076

Archer, N. A. L., Otten, W., Schmidt, S., Bengough, A. G., Shah, N., & Bonell, M. (2016). Rainfall infiltration and soil hydrological characteristics below ancient forest, planted forest and grassland in a temperate northern climate. *Ecohydrology*, *9*(4), 585–600. https://doi.org/10.1002/eco.1658

Assaye, H., Nyssen, J.,Poesen J., Lemma, H., Meshesha, D., T., Wassie, A., Adgo, E., Frankl, A., (2021). Curve number calibration for measuring impacts of land management in sub-humid Ethiopia. *Journal of Hydrology: Regional Studies (under review: EJRH-D-20-00413)*.

Beretta, A. N., Silbermann, A. V., Paladino, L., Torres, D., Bassahun, D., Musselli, R., & García-Lamohte, A. (2014). Soil texture analyses using a hydrometer: modification of the Bouyoucos method. *Cien. Inv. Agr.*, *41*(2), 263–271. https://doi.org/10.4067/S07181620201400020001 3

Bewket W. and Teferi E. (2009). Assessment of soil erosion hazard and prioritization for treatment at the watershed level: case study in the Chemoga Watershedm Blue Nile Basin, Ethiopia. Land. *Land Degrad. Develop.* 20: 609–622: *DOI: 10.1002/ldr.944*

Bewket, W., & Sterk, G. (2003). Assessment of soil erosion in cultivated fields using a survey methodology for rills in the Chemoga watershed, Ethiopia. *Agriculture, Ecosystems and Environment*, *97*(1–3), 81–93. https://doi.org/10.1016/S0167-8809(03)00127-0

Birhanu, S., & Kumsa, F. (2018). Review on Expansion of Eucalyptus, its Economic Value and Related Environmental Issues in Ethiopia. *International Journal of Research*, *4*(3), 41–46.

Borrelli, P., Robinson, D. A., Fleischer, L. R., Lugato, E., Ballabio, C., Alewell, C., … Panagos, P. (2017). An assessment of the global impact of 21st century land use change on soil erosion. *Nature Communications*, *8*(1). https://doi.org/10.1038/s41467-017-02142-7

Bruin, D., Karlberg, L., Hoff, H., Andersson, K., Binnington, T., Flores-lópez, F., Gebrehiwot, S.G., Gedif, B., Heide, F., Johnson, O., Osbeck, M., Young, C. (2015). Tackling Complexity: Understanding the Food-Energy-Environment Nexus in Ethiopia's Lake Tana Sub-basin, Water Alternatives. *8*(1), 710–734.

Chanie, T., Collick, A. S., Adgo, E., Lehmann, C. J., & Steenhuis, T. S. (2013). Eco-hydrological impacts of Eucalyptus in the semi humid Ethiopian Highlands: the Lake Tana Plain. *Journal of Hydrology and Hydromechanics*, *61*(1), 21–29. https://doi.org/10.2478/johh-2013-0004

Chen H., Liu J., Wang K., Zhang W. (2011). Spatial distribution of rock fragments on steep hillslopes in karst region of northwest. Catena 84 21–28

Colot, C. (2012). *Soil-landscape relation at regional scale in Lake Tana Basin (Ethiopia)*. MSc Thesis. Faculteit Bio-ingenieurswetenschappen, KU Leuven.

Descheemaeker, K., Poesen, J., Borselli, L., Nyssen, J., Raes, D., Haile, M., … Deckers, J. (2008). Runoff curve numbers for steep hillslopes with natural vegetation in semi-arid tropical

highlands , northern Ethiopia, *4105*(March), 4097–4105. https://doi.org/10.1002/hyp

Dessie, M., Verhoest, N. E. C., Admasu, T., Pauwels, V. R. N., Poesen, J., Adgo, E., … Nyssen, J. (2014). Effects of the floodplain on river discharge into Lake Tana (Ethiopia). *Journal of Hydrology*, *519*, 699–710.

Ebabu, K., Tsunekawa, A., Haregeweyn, N., Adgo, E., & Tsegaye, D. (2017). Analyzing the variability of sediment yield : A case study from paired watersheds in the Upper Blue Nile basin , Ethiopia Geomorphology Analyzing the variability of sediment yield : A case study from paired watersheds in the Upper Blue Nile basin , Ethiop. *Geomorphology*, *303*(March 2018), 446–455. https://doi.org/10.1016/j.geomorph.2017.12.020

Farrick, K. K., & Branfireun, B. A. (2014). Infiltration and soil water dynamics in a tropical dry forest: It may be dry but definitely not arid. *Hydrological Processes*, *28*(14), 4377–4387. https://doi.org/10.1002/hyp.10177

FAO (2015). Soil functions, soil delivery system services that enable life on Earth-Infographics. http://www.fao.org/3/ax374e/ax374e.pdf

Fenta, A. A., Tsunekawa, A., Haregeweyn, N., Poesen, J., Tsubo, M., Borrelli, P., … Kurosaki, Y. (2020). Land susceptibility to water and wind erosion risks in the East Africa region. *Science of the Total Environment*, *703*. https://doi.org/10.1016/j.scitotenv.2019.135016

Frankl, A., Nyssen, J., Adgo, E., Wassie, A., & Scull, P. (2019). Can woody vegetation in valley bottoms protect from gully erosion? Insights using remote sensing data (1938–2016) from subhumid NW Ethiopia. *Regional Environmental Change*, *19*(7), 2055–2068. https://doi.org/10.1007/s10113-019-01533-4

Gong, T., Zhu, Y., & Shao, M. (2018). Spatial distribution of caliche nodules in surface soil and their influencing factors in the Liudaogou catchment of the northern Loess Plateau, China. *Geoderma*, *329*(February), 11–19. https://doi.org/10.1016/j.geoderma.2018.05.012

Gray, B. J. R., Glysson, G. D., Turcios, L. M., & Schwarz, G. E. (2000). Comparability of Suspended-Sediment Concentration and Total Suspended Solids Data. *Usgs*, *WRI 4191*(August), 1–7.

Haregeweyn, N., Nyssen, J., Poesen, J., Schu, B., Tsunekawa, A., Nyssen, J., Tsubo, M., Meshesha

D.T., Schutt, B., Adgo, E., Tsunekawa, A., Tegegne, F. (2015). Soil erosion and conservation in Ethiopia: A review. *Progress in Physical Geography*, *39*(6), 750–774.

Haregeweyn, N., Tsunekawa, A., Poesen, J., Tsubo, M., Meshesha, D. T., Fenta, A. A., … Adgo, E. (2017). Comprehensive assessment of soil erosion risk for better land use planning in river basins: Case study of the Upper Blue Nile River. *Science of the Total Environment*, *574*, 95–108. https://doi.org/10.1016/j.scitotenv.2016.09.019

Hurni, H. (1983). Soil Erosion and Soil Formation in Agricultural Ecosystems : Ethiopia and Northern Thailand: Mountain Research and Development , May , 1983 , Vol . 3 , No . 2 , Workshop on the Stability and Instability of Mountain Ecosyst. *Mountain Research and Development*, *3*(2), 14–19.

Kassa, H., Frankl, A., Dondeyne, S., Poesen, J., & Nyssen, J. (2019). Sediment yield at southwest Ethiopia's forest frontier. *Land Degradation and Development*, *30*(6), 695–705. https://doi.org/10.1002/ldr.3260

Lemma, H., Admasu, T., Dessie, M., Fentie, D., Deckers, J., Frankl, A., … Nyssen, J. (2018). Revisiting lake sediment budgets: How the calculation of lake lifetime is strongly data and method dependent. *Earth Surface Processes and Landforms*, *43*(3), 593–607.

Lemma, H., Frankl, A., van Griensven, A., Poesen, J., Adgo, E., & Nyssen, J. (2019). Identifying erosion hotspots in Lake Tana Basin from a multisite Soil and Water Assessment Tool validation: Opportunity for land managers. *Land Degradation and Development*, *30*(12), 1449–1467.

Lemma, H., Frankl, A., Dessie, M., Poesen, J., Adgo, E., & Nyssen, J. (2020). Consolidated sediment budget of Lake Tana, Ethiopia (2012–2016). *Geomorphology*, *371*, 107434. https://doi.org/10.1016/j.geomorph.2020.107434

Li, X., Niu, J., & Xie, B. (2014). The effect of leaf litter cover on surface runoff and Soil Erosion in Northern China. *PLoS ONE*, *9*(9). https://doi.org/10.1371/journal.pone.0107789

Lv, J., Luo, H., & Xie, Y. (2019). Effects of rock fragment content, size and cover on soil erosion dynamics of spoil heaps through multiple rainfall events. *Catena*, *172*(August 2018), 179–189. https://doi.org/10.1016/j.catena.2018.08.024

Mbilinyi, B. P., Jaleta, D., Mbilinyi, B. P., Mahoo, H. F., & Lemenih, M. (2017). Effect of

Eucalyptus expansion on surface runoff in the central highlands of Ethiopia Effect of Eucalyptus expansion on surface runoff in the central highlands of Ethiopia. *Ecological Processes*, (January). https://doi.org/10.1186/s13717-017-0071-y

Minale, A. S. (2013). Population and environment interaction : the case of gilgel abbay catchment , northwestern Ethiopia. *E3 Journal of Environmental Research and Management*, *4*(1), 153–162. Retrieved from http://www.e3journals.org

MoFED. (2010). *Growth and transformation plan I (GTP I): 2011-2015*. Ethiopian Ministry of Finance and Economic Development (MoFED), Addis Ababa.

Msofe, N. K., Sheng, L., & Lyimo, J. (2019). Land use change trends and their driving forces in the Kilombero Valley Floodplain, Southeastern Tanzania. *Sustainability (Switzerland)*, *11*(2). https://doi.org/10.3390/su11020505

Nadal-Romero, E., Martínez-Murillo, J.F. , Vanmaercke, M. and Poesen, J. 2014. Corrigendum to "Scale-dependency of sediment yield from badland areas in Mediterranean environments" (Progress in Physical Geography 35 (3) (2011) 297-332). Progress in Physical Geography, 38(3):381-386

NPC. (2015). *Growth and transformation plan II (GTP II): 2015-2020*. National Planning Commission (NPC), Addis Ababa, Ethiopia.

Nyssen, J., Haile, M., Poesen, J., Deckers, J., & Moeyersons, J. (2001). Removal of rock fragments and its effect on soil loss and crop yield, Tigray, Ethiopia. https://doi.org/10.1079/SUM200173

Nyssen, J., Poesen, J., Lanckriet, S., Jacob, M., Moeyersons, J., Haile, M., … Deckers, J. (2015). Land degradation in the Ethiopian Highlands. In P. Billi (Ed.), *Landscapes and Landforms of Ethiopia* (pp. 369–385). Springer, The Netherlands.

Nyssen, J., Poesen, J., Moeyersons, J., Haile, M., & Deckers, J. (2008). Dynamics of soil erosion rates and controlling factors in the Northern Ethiopian highlands – towards a sediment budget. *Earth Surface Processes and Landforms*, *33*(5), 695–711.

Olubanjo, O. O. (2017). Evaluation of the Effect of Soil Physico-Chemical Properties on Erodibility and Infiltration. *Journal of Sustainable Technology*, *8*(1). Retrieved from www.jost.futa.edu.ng

Oostwoud Wijdenes, D., Poesen, J., Vandekerckhove, L. and de Luna, E. 1997. Chiselling effects

on the vertical distribution of rock fragments in the tilled layer of a Mediterranean soil. Soil and Tillage Research, 44:55-66.

Poesen, J. (2018). Soil erosion in the Anthropocene: Research needs. *Earth Surf. Process. Landforms*, *43*(1), 64–84.

Poesen, J. W., Van Wesemael, B., Bunte, K., & Benet, A. S. (1998). Variation of rock fragment cover and size along semiarid hillslopes: a case-study from southeast Spain. *Geomorphology*, *23*(2–4), 323–335. https://doi.org/10.1016/S0169-555X(98)00013-0

Poesen, J., & Lavee, H. (1994). Rock fragments in top soils : significance and processes. *Catena*, *23*, 1–28.

Poesen, J. W., Torri, D., & Bunte, K. (1994). Effects of rock fragments on soil erosion by water at different spatial scales: a review. *Catena*, *23*(1–2), 141–166. https://doi.org/10.1016/0341-8162(94)90058-2

Poppe, L., Frankl, A., Poesen, J., Admasu, T., Dessie, M., Adgo, E., … Nyssen, J. (2013). Geomorphology of the Lake Tana Basin, Ethiopia. *Journal of Maps*, *9*, 431–437.

R Core Team. (2020). R: A language and environment for statistical computing. R Foundation for Statistical Computing, Vienna, Austria.

Rodríguez-Blanco, M. L., Taboada-Castro, M. M., & Taboada-Castro, M. T. (2012). Réponse pluie-débit et coefficients de ruissellement événementiels dans une région humide (nordouest de l'Espagne). *Hydrological Sciences Journal*, *57*(3), 445–459. https://doi.org/10.1080/02626667.2012.666351

Sajikumar, N., & Remya, R. S. (2015). Impact of land cover and land use change on runoff characteristics. *Journal of Environmental Management*, *161*, 460–468. https://doi.org/10.1016/j.jenvman.2014.12.041

Shen, J. (1981). Discharge characteristics of triangular-notch thin-plate weirs. *Geological Survey Water-Supply Paper 1617-B*, 62.

Smets, T., Poesen, J. & Bochet, E. 2008. Impact of plot length on the effectiveness of different soil-surface covers in reducing runoff and soil loss by water. Progress in Physical Geography 32(6):654-677 (DOI: 10.1177/0309133308101473).

Steenhuis, T. S., Collick, A. S., Easton, Z. M., Leggesse, E. S., Bayabil, H. K., White, E. D., …

Ahmed, A. A. (2009). Predicting discharge and sediment for the Abay (Blue Nile) with a simple model. *Hydrological Processes*, *23*(26), 3728–3737. https://doi.org/10.1002/hyp.7513

Storey, R., Parkyn, S., Smith, B., Croker, G., & Franklin, P. (2009). Effects of Development on Zero-order Streams in the Waikato Region. *Environment Waikato Technical Report 2009/22*, *22*.

Tamene, L., Sileshi, G. W., Ndengu, G., Mponela, P., Kihara, J., Sila, A., & Tondoh, J. (2019). Soil structural degradation and nutrient limitations across land use categories and climatic zones in Southern Africa. *Land Degradation and Development*, *30*(11), 1288–1299. https://doi.org/10.1002/ldr.3302

Taye, G., Poesen, J., Van Wesemael, B., Vanmaercke, M., Teka, D., Deckers, J., Goosse, T., Maetens, W., Nyssen, J., Hallet, V., Haregeweyn, N. 2013. Effects of land use, slope gradient, and soil and water conservation structures on runoff and soil loss in semi-arid Northern Ethiopia. Physical Geography 34(3):236-258. (http://dx.doi.org/10.1080/02723646.2013.832098).

Teklemariam, D., Azadi, H., Nyssen, J., Haile, M., & Witlox, F. (2016a). How sustainable is transnational farmland acquisition in Ethiopia? Lessons learned from the Benishangul-Gumuz Region. *Sustainability (Switzerland)*, *8*(3). https://doi.org/10.3390/su8030213

Teklemariam, D., Azadi, H., Nyssen, J., Haile, M., & Witlox, F. (2016b). How sustainable is transnational farmland acquisition in Ethiopia? Lessons learned from the Benishangul-Gumuz Region. *Sustainability (Switzerland)*, *8*(3), 1–27. https://doi.org/10.3390/su8030213

Temesgen, G., Amare, B., & Abraham, M. (2014). Population dynamics and land use/land cover changes in Dera District, Ethiopia. *Global Journal of Biology, Agriculture & Health Sciences*, *3*(1), 134–140.

Tilahun, S. A., Guzman, C. D., Zegeye, A. D., Dagnew, D. C., Collick, A. S., Yitaferu, B., & Steenhuis, T. S. (2015). Distributed discharge and sediment concentration predictions in the sub-humid Ethiopian highlands: The Debre Mawi watershed. *Hydrological Processes*, *29*(7), 1817–1828. https://doi.org/10.1002/hyp.10298

Tsuboyama, Y., Sidle, R. C., Noguchi, S., Murakami, S., & Shimizu, T. (2000). A zero-order basin - its contribution to catchment hydrology and internal hydrological processes. *Hydrological Processes*, *14*(3), 387–401. https://doi.org/10.1002/(SICI)1099-1085(20000228)14:3<387::AID-HYP944>3.0.CO;2-Q

Wakiyama, Y., Onda, Y., Nanko, K., Mizugaki, S., Kim, Y., Kitahara, H., & Ono, H. (2010). Estimation of temporal variation in splash detachment in two Japanese cypress plantations of contrasting age. *Earth Surface Processes and Landforms*, *35*(9), 993–1005. https://doi.org/10.1002/esp.1844

Walkley, A., & Black, I. A. (1934). An examination of the degtjareff method for determining soil organic matter, and a proposed modification of the chromic acid titration method. *Soil Science*, *37*(1), 29–38. https://doi.org/10.1097/00010694-193401000-00003

Wassie, S. B. (2020). Natural resource degradation tendencies in Ethiopia: a review. *Environmental Systems Research*, *9*(1), 1–29. https://doi.org/10.1186/s40068-020-00194-1

Wolka, K., Mulder, J., & Biazin, B. (2018). Effects of soil and water conservation techniques on crop yield, runoff and soil loss in Sub-Saharan Africa: A review. *Agricultural Water Management*, *207*, 67–79: https://doi.org/10.1016/j.agwat.2018.05.016

Wuepper, D., Borrelli, P., & Finger, R. (2020). Countries and the global rate of soil erosion. *Nature Sustainability*, *3*(1), 51–55. https://doi.org/10.1038/s41893-019-0438-4

Yimer, F., Messing, I., Ledin, S., & Abdelkadir, A. (2008). Effects of different land use types on infiltration capacity in a catchment in the highlands of Ethiopia. *Soil Use and Management*, *24*(4), 344–349. https://doi.org/10.1111/j.1475-2743.2008.00182.x

Zeleke, G., & Hurni, H. (2001). Implications of Land Use and Land Cover Dynamics for Mountain Resource Degradation in the Northwestern Ethiopian Highlands Implications of Land Use and Land Cover Dynamics for Mountain Resource Degradation in the Northwestern Ethiopian Highlands, *21*(2), 184–191.

## List of tables

**TABLE 1** Physical characteristics of the studied catchments. *RFC* is rock fragment cover, *SOM* is soil organic matter content, '*Feses*' is a seasonal drainage system that farmers prepare with deep furrowing to facilitate smooth runoff and reduce potential sheet erosion, BDL is badlands, CR is croplands, GR is grazing, NF is natural forest, and PL is plantation

| ID | Land use types | Area ($m^2$) | Mean slope gradient (%) | Slope length (m) | Stone bund density (m $ha^{-1}$) | *Feses* density (m $ha^{-1}$) | *RFC* (%) | *SOM* (%) | Soil depth (cm) | Texture (%) | | |
|---|---|---|---|---|---|---|---|---|---|---|---|---|
| | | | | | | | | | | Sand | Silt | Clay |
| BDL1 | Badland | 520 | 22 | 34 | 0 | 0 | 3 | 1.8 | 50 | 59 | 17 | 24 |
| BDL2 | Badland | 546 | 26 | 28 | 0 | 0 | 2 | 3.7 | 50 | 44 | 20 | 36 |
| CR4 | Cropland | 1715 | 13 | 30 | 196 | 1389 | 20 | 2.2 | 50 | 45 | 18 | 37 |
| CR5 | Cropland | 716 | 28 | 32 | 336 | 489 | 40 | 4.4 | 15 | 74 | 12 | 14 |
| CR1 | Cropland | 1205 | 12 | 11.5 | 896 | 855 | 20 | 3.4 | 40 | 52 | 22 | 26 |
| CR2 | Cropland | 1354 | 10 | 15.5 | 625 | 591 | 70 | 3.7 | 50 | 48 | 28 | 24 |
| CR3 | Cropland | 578 | 25 | 28 | 554 | 1211 | 35 | 4.5 | 50 | 46 | 22 | 32 |
| GR1 | Grazing land | 534 | 23 | 26 | 0 | 0 | 30 | 3.7 | 40 | 40 | 12 | 48 |
| GR2 | Grazing land | 634 | 20 | 32 | 0 | 0 | 2 | 3.3 | >100 | 52 | 20 | 28 |
| NF1 | Natural forest | 682 | 22 | 31 | 0 | 0 | 3 | 10.5 | 50 | 66 | 24 | 10 |
| NF2 | Natural forest | 520 | 19 | 27 | 0 | 0 | 4 | 10.4 | 50 | 60 | 26 | 14 |
| NF3 | Natural forest | 760 | 9 | 28 | 0 | 0 | 4 | 5.0 | 40 | 64 | 22 | 14 |
| PL1 | Plantation (Eucalypt) 8canopy | 324 | 11 | 33 | 0 | 0 | 5 | 4.0 | >100 | 44 | 18 | 38 |
| PL2 | Plantation (Eucalypt) | 566 | 10 | 37 | 0 | 0 | 6 | 3.7 | >100 | 46 | 20 | 34 |

**TABLE 2** Event summary of results: mean event rainfall (*P*), mean event suspended sediment concentration (*SSC*), mean event sediment yield (*SY*), mean event runoff depth ($RO_d$), number of measured rainfall-runoff events (n) for the different catchments (ID). Values in parentheses are standard deviation

| ID | n | | *P* (mm) | | $I_{30}$ | | *SSC* (g $l^{-1}$) | | *SY* (kg $ha^{-1}$) | | $RO_d$ (mm) | |
|---|---|---|---|---|---|---|---|---|---|---|---|---|
| | 2018 | 2019 | 2018 | 2019 | 2018 | 2019 | 2018 | 2019 | 2018 | 2019 | 2018 | 2019 |
| BDL1 | 20 | 24 | 5.9(1.1) | 8.5(1.3) | 37.2 | 56.4 | 5.8(1) | 7.1(0.4) | 202(67) | 429(96) | 3.5(0.9) | 5.1(0.9) |
| BDL2 | 14 | 23 | 7.7(1.4) | 6.9(1.6) | 37.2 | 56.4 | 6.1(1.6) | 3.5(0.7) | 301(101) | 337(222) | 4.6(0.7) | 3.8(1.4) |
| CR4 | 18 | 24 | 6.1(0.8) | 8.1(1.4) | 37.2 | 56.4 | 3.8(0.6) | 5.2(0.6) | 131(38) | 164(60) | 3.1(0.6) | 2.1(0.6) |
| CR5 | 20 | 28 | 10.0(1.3) | 12.2(1.5) | 44.4 | 43.6 | 2.8(0.5) | 4.1(0.3) | 99 (36) | 152(48) | 2.6(0.5) | 2.7(0.6) |
| CR1 | 23 | 27 | 12.2(2.2) | 13.6(1.6) | 58.4 | 49.2 | 2.7(0.4) | 2.4(0.3) | 151(34) | 134(45) | 7.1(1.7) | 3.1(0.7) |
| CR2 | 20 | 32 | 11.8(2.0) | 12.7(1.4) | 13.2 | 42.0 | 1.9(0.3) | 4.6(0.3) | 120(36) | 365(119) | 6.0(1.3) | 5.5(1.1) |
| CR3 | 26 | 41 | 7.2(1.0) | 8.5(1.3) | 37.2 | 56.4 | 4.3(0.6) | 4.0(0.2) | 106(48) | 192(69) | 1.8(0.7) | 3.4(0.8) |
| GR1 | 19 | 34 | 7.3(1.0) | 10.2(1.4) | 37.2 | 56.4 | 4.0(0.7) | 1.4(0.1) | 133(25) | 81(19) | 3.6(0.5) | 4.7(0.8) |
| GR2 | 12 | 33 | 10.1(1.8) | 12.0(1.4) | 44.4 | 43.6 | 0.3(0.1) | 0.4(0.0) | 14(2.4) | 40(11) | 4.7(0.9) | 6.4(1.2) |
| NF1 | 6 | 24 | 12.5(3.1) | 7.8(1.6) | 37.2 | 56.4 | 2.5(1.0) | 0.7(0.2) | 4.8(2.1) | 6.4(3.6) | 0.3(0.1) | 0.3(0.2) |
| NF2 | 14 | 20 | 8.0(1.7) | 8.8(1.9) | 37.2 | 56.4 | 2.0(0.2) | 0.5(0.2) | 5.5(2) | 2.0(1.0) | 0.4(0.2) | 0.1(0.1) |
| NF3 | 21 | 34 | 11.8(2.1) | 10.6(1.2) | 58.4 | 49.2 | 2.4(0.3) | 1.8(0.0) | 22.0(6) | 13.7(2.5) | 0.9(0.2) | 0.7(0.1) |
| PL1 | 9 | 16 | 12.0(2.6) | 11.5(2.7) | 58.4 | 49.2 | 0.7(0.3) | 1.8(0.0) | 8.6(5.3) | 69(30) | 1.1(0.5) | 3.3(0.1) |
| PL2 | 4 | 32 | 9.0(2.0) | 11.3(1.4) | 44.4 | 43.6 | 2.2(0.3) | 0.3(0.0) | 55(21) | 21(4.7) | 2.2(0.6) | 4.7(0.1) |

Note: For details of the catchments ID see Table 1

**TABLE 3** Rating curve parameters for ( $SSC_i$ [g $l^{-1}$] = a$Q_i$ [$m^3$ $S^{-1}$] + b), n = number of runoff events for catchments (ID)

| ID | a | b | $R^2$ | n | p |
|---|---|---|---|---|---|
| BDL1 | 707.300 | 5.235 | 0.43 | 48 | <0.01 |
| BDL2 | 1028.879 | 1.625 | 0.75 | 15 | <0.01 |
| CR4 | 526.753 | 4.599 | 0.70 | 31 | <0.01 |
| CR5 | 978.402 | 2.595 | 0.61 | 25 | <0.01 |
| CR1 | 868.331 | 0.560 | 0.46 | 30 | <0.01 |
| CR2 | 515.974 | 2.771 | 0.20 | 35 | <0.01 |
| CR3 | 452.310 | 3.530 | 0.11 | 51 | 0.016 |
| GR1 | 203.462 | 1.088 | 0.45 | 47 | <0.01 |
| GR2 | 45.775 | 0.251 | 0.20 | 37 | <0.01 |
| NF1 | 469.753 | 1.615 | 0.55 | 16 | <0.01 |
| NF2 | 22624.819 | 1.965 | 0.62 | 5 | 0.11 |
| NF3 | 469.753 | 1.615 | 0.55 | 16 | <0.01 |
| PL1 | 293.032 | 0.195 | 0.73 | 17 | <0.01 |
| PL2 | 56.253 | 0.224 | 0.40 | 39 | <0.01 |

Note: For details of the catchments ID see Table 1

**TABLE 4** Frequency of events above the event tolerance limit threshold for the different catchments (ID)

| ID | Number of events | Number of events over the threshold | Number of events below the threshold | % events above the threshold |
|---|---|---|---|---|
| BDL1 | 44 | 42 | 2 | 95 |
| BDL2 | 37 | 33 | 4 | 89 |
| CR1 | 50 | 23 | 27 | 46 |
| CR2 | 52 | 13 | 39 | 25 |
| CR3 | 67 | 54 | 13 | 81 |
| CR4 | 42 | 32 | 10 | 76 |
| CR5 | 48 | 38 | 10 | 79 |
| GR1 | 53 | 21 | 32 | 40 |
| GR2 | 45 | 0 | 45 | 0 |
| PL1 | 25 | 0 | 25 | 0 |
| PL2 | 36 | 2 | 34 | 6 |
| NF1 | 30 | 0 | 30 | 0 |
| NF2 | 34 | 0 | 34 | 0 |
| NF3 | 55 | 0 | 55 | 0 |

Note: For ID details see Table

## List of figures

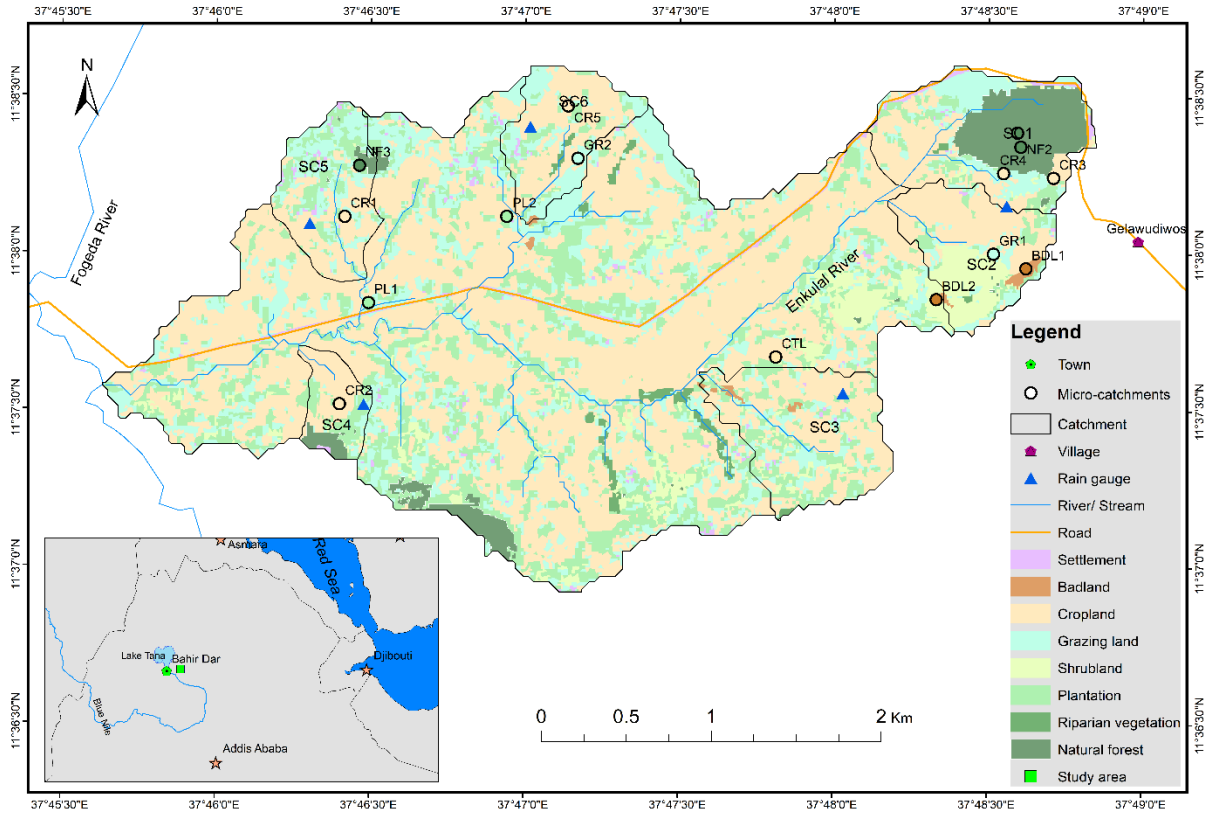


**FIGURE 2** Land use in the Enkulal Catchment and the location of the rain gauges and study catchments; Map prepared using the sentinel-2 satellite image of the scene in February, 2019 from the Copernicus open access hub (https://scihub.copernicus.eu/) and manual digitization using google earth and Q-GIS

**FIGURE 2** V-notch weir cut from a plastic jar allowing one to measure runoff and sediment yield in micro-catchments at low cost and low risk (at CR2).

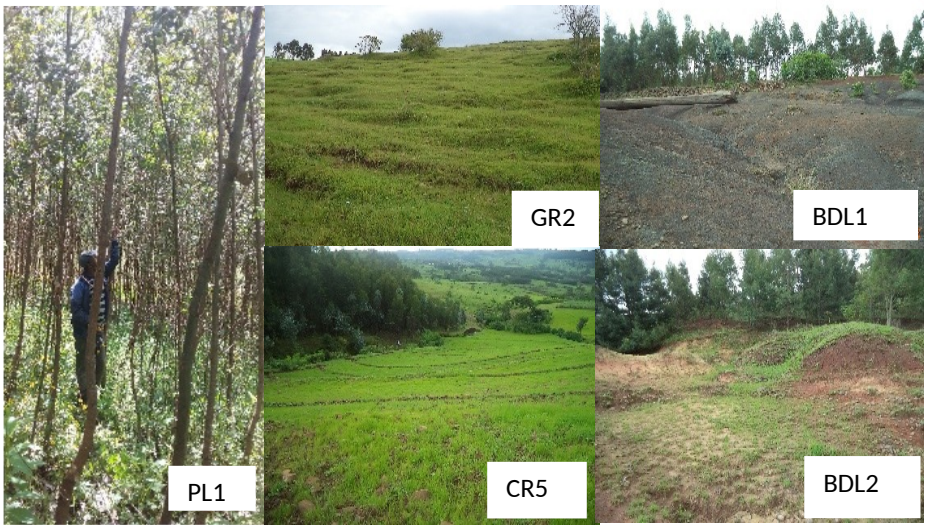


**FIGURE 3** Illustration of the land use in some of the studied micro-catchments; PL1 is Eucalyptus plantation, GR2 is grazing land (cut-and-carry), BDL1 is badland completely bare, BDL2 is rehabilitating badland, CR5 is cropland

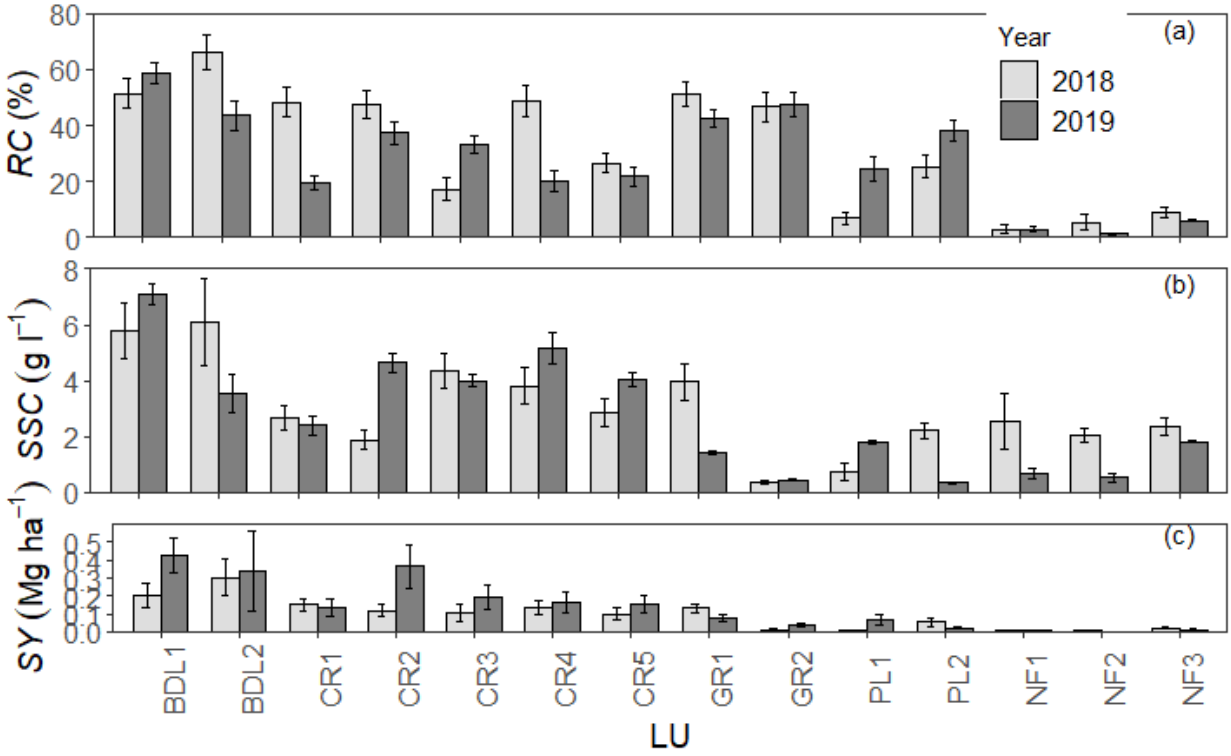


**FIGURE 4** Average event runoff coefficient (*RC*) (a), suspended sediment concentration (*SSC*) (b), and event sediment yield (*SY*) (c) for the different catchments (ID, for details see Table 1)

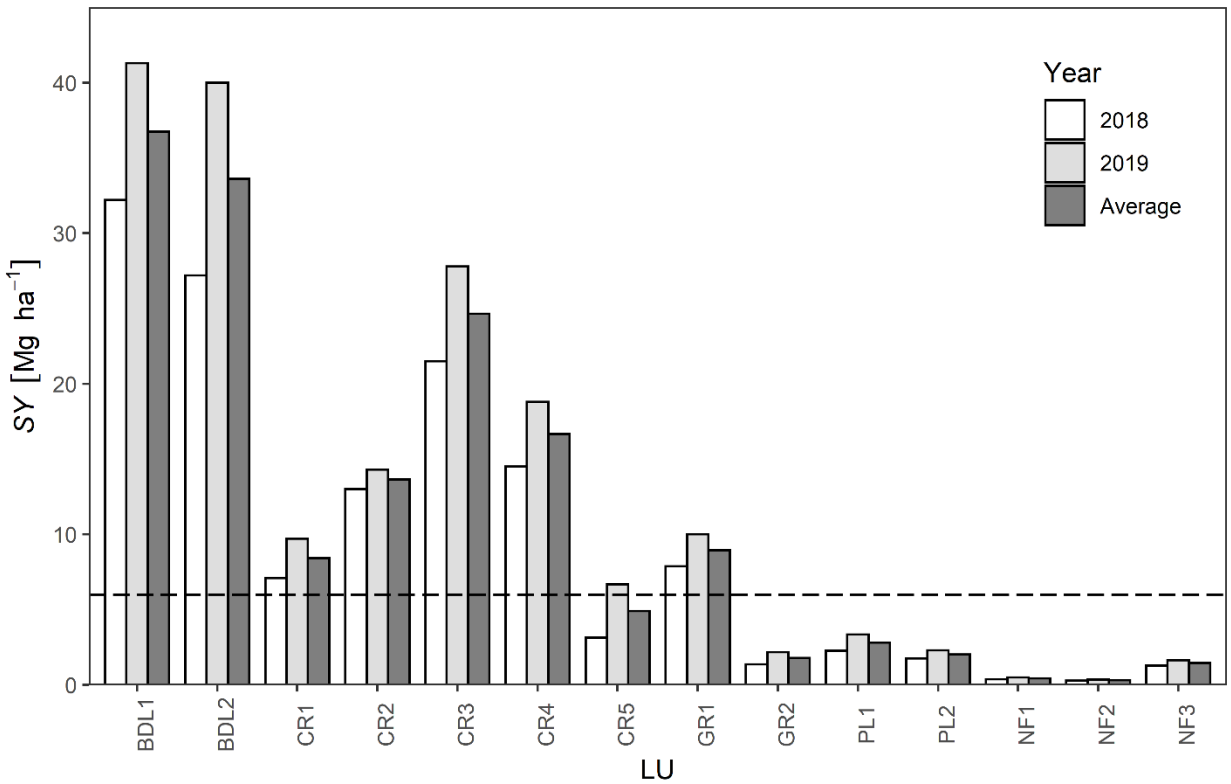

**FIGURE 5** Annual sediment yield (*SY*, Mg ha$^{-1}$) of the different catchments (ID, see Table 1); the dash line represents the soil loss tolerance limit for the highlands of Ethiopia for equivalent elevation of our study area (6 ton ha$^{-1}$ year$^{-1}$) adopted from Hurni (1983)

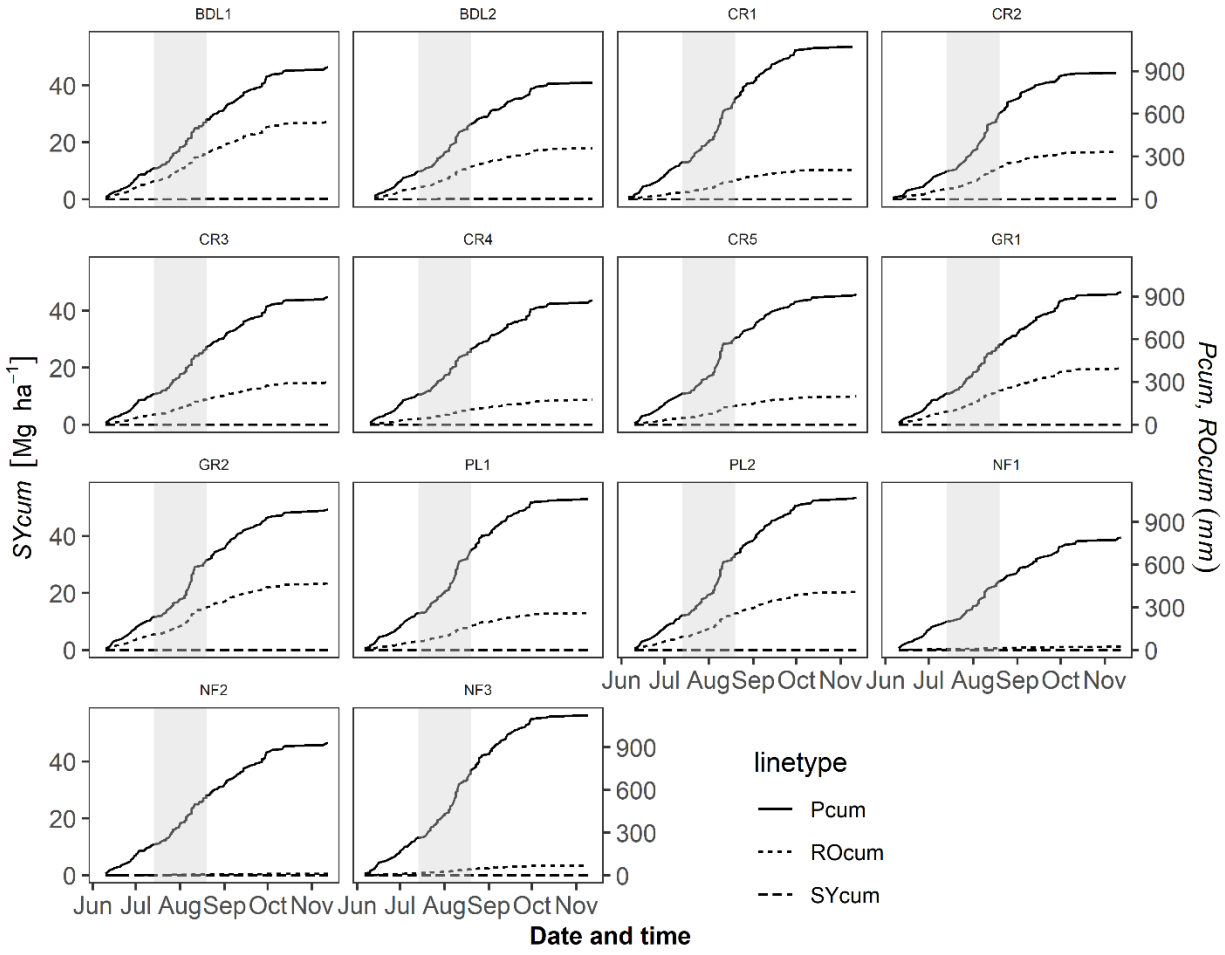


**FIGURE 6** Cumulative event rainfall (*P*cum, mm), cumulative event runoff (*RO*cum, mm), cumulative event sediment yield (*SY*, Mg ha$^{-1}$) for the different catchments (ID) of the 2019 rainy season (for more details see Table 1). Grey-shaded period indicates the steepest gradient in the curves

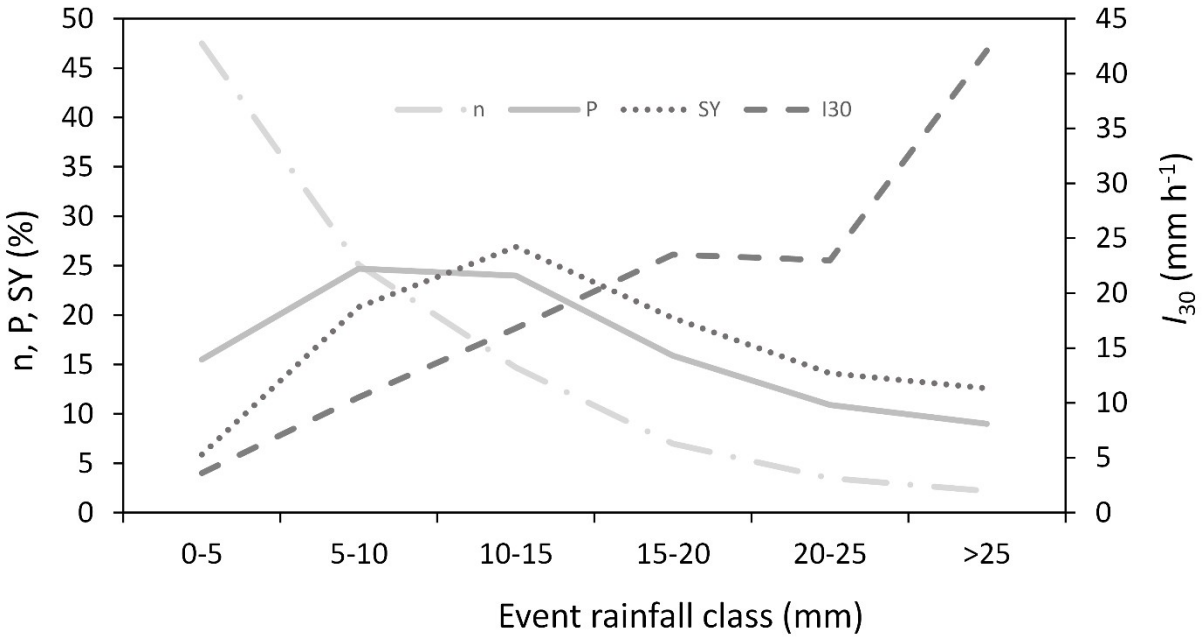


**FIGURE 7** The percentage of the number of events (*n*), rainfall depth (*P*, mm), sediment yield (*SY*, Mg ha$^{-1}$ yr$^{-1}$) and average event maximum 30 minute intensity ($I_{30}$, mm h$^{-1}$) in the different event rainfall classes

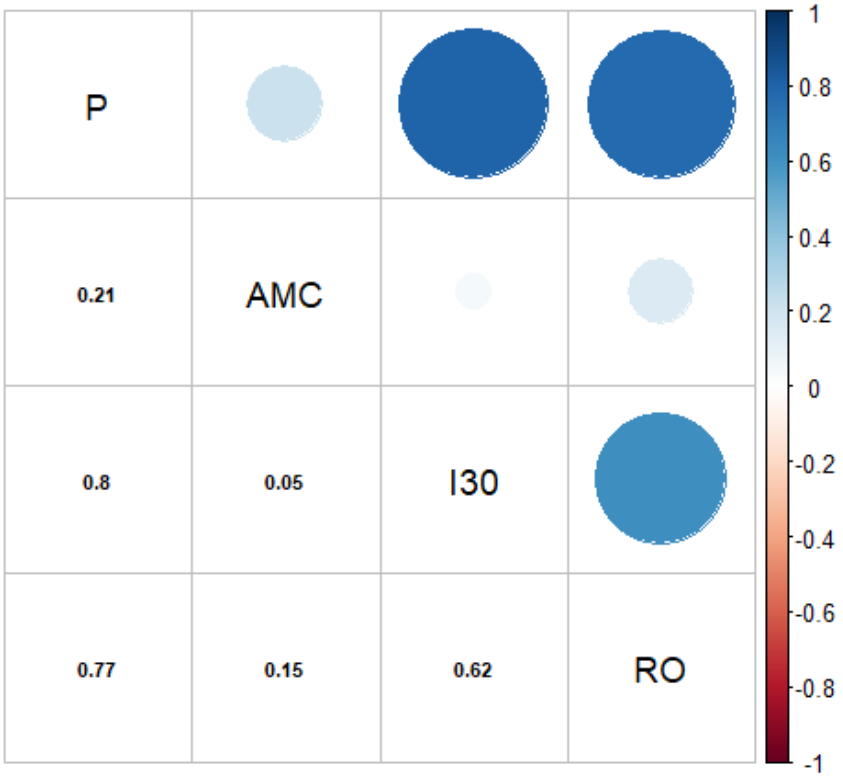

**FIGURE 8** Correlation coefficient between the event rainfall ($P$, mm), runoff ($RO_d$, mm), antecedent moisture condition ($AMC$, mm), 30-minute maximum intensity ($I_{30}$, mm $h^{-1}$) variables; the darker the tone of the color and the bigger the size of the circle both indicate strong correlation, while the blue color is for positive correlation, the red color is for negative correlation. Besides, any significant correlation with p-value < 0.01 is indicated with the circular and when it is not significant it remains blank

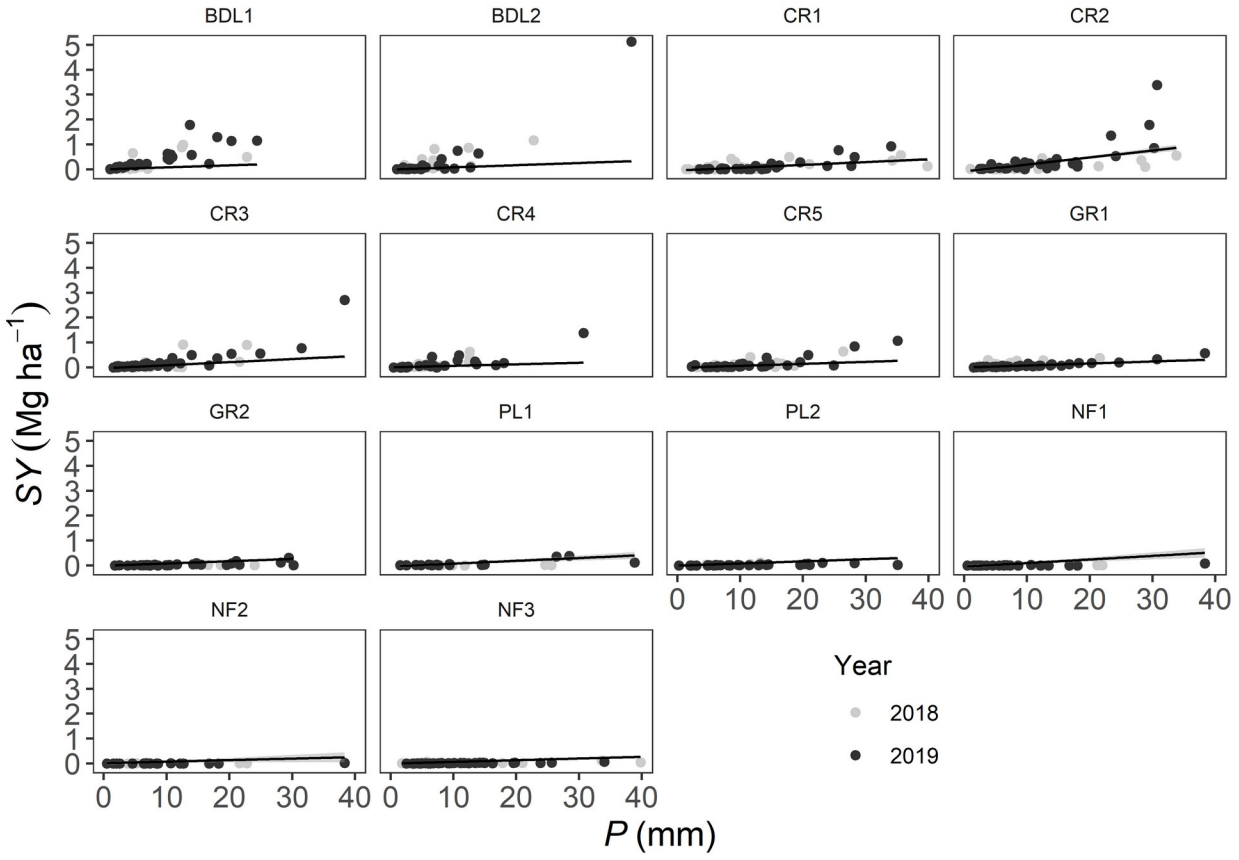


**FIGURE 9** A scatter plot of event sediment yield ($SY$, Mg $ha^{-1}$) and corresponding event rainfall ($P$, mm) for the different catchments (ID); the black line is a threshold for the tolerance limit. For ID details see Table 1

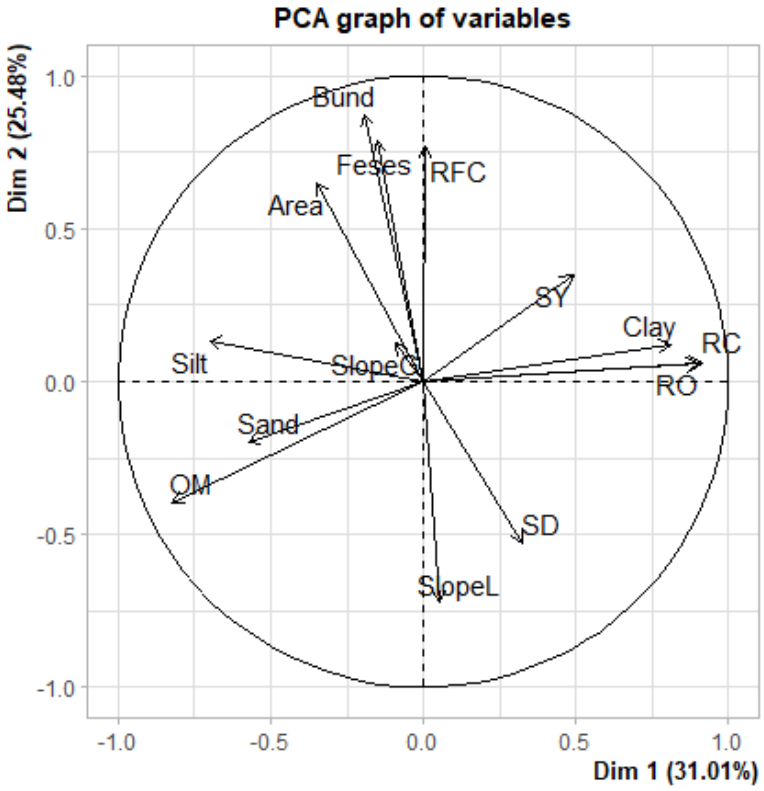


**FIGURE 10** Principal component analysis (*PCA*) biplot for catchment characteristics

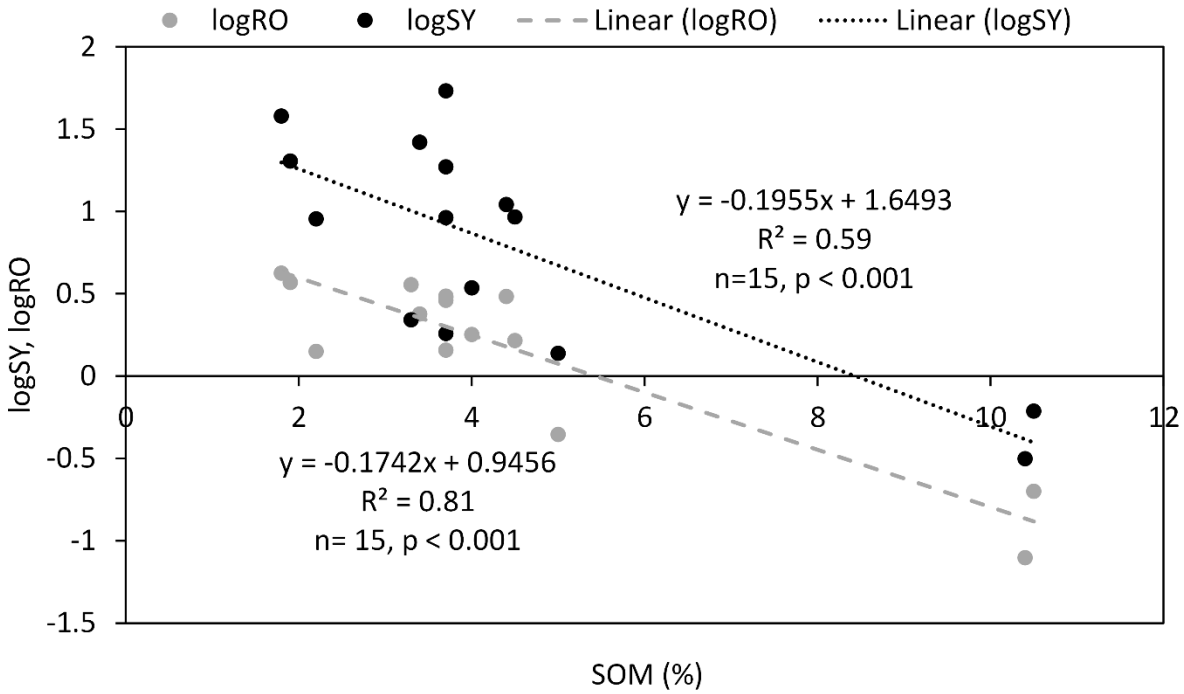

**FIGURE 11** Effect of soil organic matter (*SOM, %*) on event mean runoff depth ($RO_{d,}$ mm) and annual sediment yield (*SY,* Mg ha$^{-1}$ yr$^{-1}$) (log transformed)

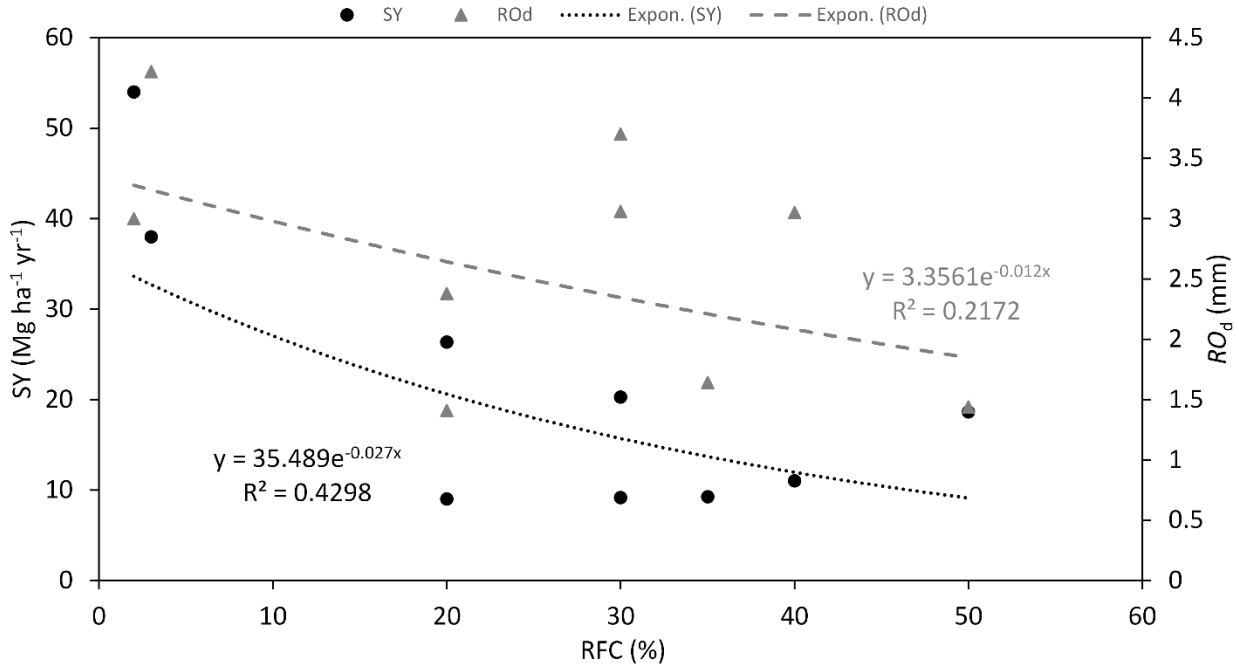


**FIGURE 12** Effect of rock fragment cover (*RFC*) on event mean runoff depth ($RO_{d,}$ grey) and mean annual sediment yield (*SY,* dark black)

**FIGURE 13** Exposure of tree roots with known age (in this particular example an exposed root from a 5 year old *Grevilia robusta* tree) 16 cm above the current soil surface; a proxy for estimating rate of annual soil erosion rate and corresponding *SY* for badlands, at BDL2, 2020

## Appendix

**Annex A.** Rating curve for event rainfall depth (mm) and event sediment yield (kg $ha^{-1}$)

| MC | a | b | $R^2$ | n | p |
|---|---|---|---|---|---|
| BDL1 | 52.729 | -60.004 | 0.59 | 42 | <0.01 |
| BDL2 | 109.12 | -464.74 | 0.76 | 35 | <0.01 |
| CR_PL1 | 33.012 | -90.803 | 0.61 | 40 | <0.01 |
| CR_PL2 | 24.173 | -142.296 | 0.61 | 46 | <0.01 |
| CR1 | 14.61 | -47.804 | 0.44 | 48 | <0.01 |
| CR2 | 41.27 | -237.06 | 0.4 | 50 | <0.01 |
| CR3 | 42.293 | -88.3 | 0.65 | 65 | <0.01 |
| CTL | 30.413 | -75.607 | 0.53 | 58 | <0.01 |
| GR1 | 11.379 | -4.334 | 0.56 | 51 | <0.01 |
| GR2 | 4.7841 | -21.9544 | 0.43 | 43 | <0.01 |
| NF1 | 1.3931 | -6.1226 | 0.51 | 28 | <0.01 |
| NF2 | 0.399 | 0.2019 | 0.23 | 32 | 0.004 |
| NF3 | 1.7661 | -2.5815 | 0.5 | 53 | <0.01 |
| PL1 | 6.317 | -26.483 | 0.37 | 23 | 0.001 |
| PL2 | 2.4014 | -2.215 | 0.38 | 34 | <0.01 |

**Annex B**. Summary of result of analysis of variance for *RC* (%) and *SSC*(g $l^{-1}$) in the different land use types, to the right upper side is for *SSC* and to the left bottom is *RC*.

| MC | BDL1 | BDL2 | CR4 | CR5 | CR1 | CR2 | CR3 | CTL | GR1 | GR2 | NF1 | NF2 | NF3 | PL1 | PL2 |
|---|---|---|---|---|---|---|---|---|---|---|---|---|---|---|---|
| **BDL1** | | ns | * | *** | *** | *** | *** | *** | *** | *** | *** | *** | *** | *** | *** |
| **BDL2** | * | | *** | *** | *** | *** | *** | *** | *** | *** | *** | *** | *** | *** | *** |
| **CR4** | *** | ** | | *** | * | ns | * | ns | * | *** | *** | *** | *** | *** | *** |
| **CR5** | *** | *** | ns | | ns | ** | ns | *** | ns | ns | ns | ns | ns | ns | ns |
| **CR1** | *** | *** | ns | ns | | ns | *** | *** | ns | ns | * | * | ns | ns | ns |
| **CR2** | * | ns | ns | *** | ns | | *** | ns | ns | *** | *** | *** | *** | *** | *** |
| **CR3** | * | ** | ns | ns | ns | ** | | ns | *** | *** | *** | *** | *** | *** | *** |
| **CTL** | ns | ns | *** | *** | *** | ** | *** | | *** | *** | *** | *** | *** | *** | *** |
| **GR1** | ns | ns | ns | *** | ns | ns | *** | ns | | ns | * | * | * | ns | ns |
| **GR2** | ns | ns | ** | *** | * | ns | *** | ns | ns | | ns | ns | ns | ns | ns |
| **NF1** | *** | *** | *** | *** | *** | *** | *** | *** | *** | *** | | ns | ns | ns | ns |
| **NF2** | *** | *** | *** | *** | *** | *** | *** | *** | *** | *** | ns | | ns | ns | ns |
| **NF3** | *** | *** | *** | ** | *** | *** | *** | *** | *** | *** | ns | ns | | ns | ns |
| **PL1** | *** | *** | ns | ns | ns | *** | ns | ns | * | ** | ns | ns | ns | | ns |
| **PL2** | ** | *** | ns | ns | ns | ns | ns | ns | ns | ns | *** | ** | ** | Ns | |

**Note:** * represent significance for *RC* (* $p < 0.05$, ** $p < 0.01$, *** $p < 0.001$), left bottom
*represent significance for *SSC* (* $p < 0.05$, ** $p < 0.01$, ***$p < 0.001$), right up
$^{ns}$ represent not significant

**Annex C**: Crop calendar of the crops grown in the croplands of the selected micro-catchments

| Cropland | Year | Crop | Mar | Apr | May | Jun | Jul | Aug | Sep | Oct | Nov |
|---|---|---|---|---|---|---|---|---|---|---|---|
| CR1 | 2018 | Teff | | | | | | | | | |
| | 2019 | Maize | | | | | | | | | |
| CR2 | 2018 | Maize | | | | | | | | | |
| | 2019 | Teff | | | | | | | | | |
| CR3 | 2018 | Wheat | | | | | | | | | |
| | 2019 | Teff | | | | | | | | | |
| CR4 | 2018 | Teff | | | | | | | | | |
| | 2019 | Euc. | | | | | | | | | |
| CR5 | 2018 | Teff | | | | | | | | | |
| | 2019 | Euc. | | | | | | | | | |

Ploughing | Cleaning | Sowing | Weeding | Harvesting | Planting